THE ASTROPHYSICAL JOURNAL, 470:L73–L76, 1996 October 10


# LABORATORY MEASUREMENTS OF Fe XXIV *L*-SHELL LINE EMISSION

D. W. SAVIN,[1,2] P. BEIERSDORFER,[3] J. CRESPO LÓPEZ-URRUTIA,[3] V. DECAUX,[3] E. M. GULLIKSON,[4]
S. M. KAHN,[1,2] D. A. LIEDAHL,[3] K. J. REED,[3] AND K. WIDMANN[3]

*Received 1996 June 18; accepted 1996 August 2*

## ABSTRACT

Recent *ASCA* spectra exhibit discrepancies with the relative line intensities of various Fe XXIII and XXIV *L*-shell emission lines predicted by standard plasma emission codes. To address this issue, we have carried out a series of high-resolution, broadband measurements of Fe XXIV line emission using an electron beam ion trap facility. X-ray lines produced in the trap are detected and resolved using Bragg crystal spectrometers. We report measurements of $3 \rightarrow 2$ and $4 \rightarrow 2$ transitions, which result primarily from electron impact excitation. Overall, good agreement is found with distorted wave calculations.

*Subject headings:* atomic data — atomic processes — methods: laboratory — X-rays: general

## 1. INTRODUCTION

Recent *ASCA* observations in the 0.7–2.0 keV spectral band exhibit discrepancies with model predictions using standard plasma emission codes (Drake et al. 1994; Fabian et al. 1994; White et al. 1994). These discrepancies suggest errors in the atomic data used in the codes. This is most clearly seen in the *ASCA* spectrum of the Centaurus cluster of galaxies (Fabian et al. 1994) where the $(4 \rightarrow 2)/(3 \rightarrow 2)$ line ratio for the principal Fe XXIII and XXIV *L*-shell transitions is substantially lower than predicted by the RS (Raymond & Smith 1977 and updates) and the MEKA (Mewe, Gronenschild, & van den Oord 1985; Kaastra & Mewe 1993) codes. Liedahl, Osterheld, & Goldstein (1995) have calculated new electron impact excitation (EIE) rate coefficients and find $(4 \rightarrow 2)/(3 \rightarrow 2)$ line ratios ~2–3 times smaller than in the RS and MEKA codes. While this appears to provide better agreement with the *ASCA* data, their calculations yield Fe XXIII and XXIV $(4 \rightarrow 2)/(3 \rightarrow 2)$ line ratios that are still ~2 times larger than observed in solar flares (McKenzie et al. 1985). Understanding these line emissivities is also expected to be important for accurately interpreting spectroscopic data collected by *AXAF*, *XMM*, and *Astro-E* where these lines will be observed routinely from stellar coronae, supernova remnants, and clusters of galaxies.

To address these issues, we have carried out broadband, high-resolution measurements of Fe XXIV $3 \rightarrow 2$ and $4 \rightarrow 2$ line emission using the Lawrence Livermore electron beam ion trap (EBIT; Levine et al. 1988). EBIT was operated at electron beam energies where EIE from the ground level dominates the excitation of these lines. Here we present line ratio measurements for the $3p\ ^2P_{3/2} \rightarrow 2s\ ^2S_{1/2}$ (λ10.62), $3d\ ^2D_{5/2} \rightarrow 2p\ ^2P_{3/2}$ (λ11.17), and $4p\ ^2P_{3/2,1/2} \rightarrow 2s\ ^2S_{1/2}$ (λ7.99) transitions, all relative to the $3p\ ^2P_{1/2} \rightarrow 2s\ ^2S_{1/2}$ (λ10.66) transition (hereafter, $3p_{3/2}$–$2s_{1/2}$, $3d_{5/2}$–$2p_{3/2}$, $4p_{3/2,1/2}$–$2s_{1/2}$, and $3p_{1/2}$–$2s_{1/2}$, respectively).

[1] Departments of Physics and Astronomy and Space Sciences Laboratory, University of California, Berkeley, CA 94720.
[2] Current address: Department of Physics and Columbia Astrophysics Laboratory, Columbia University, New York, NY 10027.
[3] Lawrence Livermore National Laboratory, Livermore, CA 94550.
[4] Lawrence Berkeley National Laboratory, Berkeley, CA 94720.

## 2. EXPERIMENTAL APPROACH

EBIT uses a magnetically confined beam of electrons to produce and trap ions (Levine et al. 1988). The diameter of the beam is ~60 μm. The electron beam may be used to excite the trapped ions. The energy spread of the beam is approximately Gaussian with a FWHM of ~50 eV. The ion temperature is ~600 eV for operating parameters typical of EBIT spectroscopy measurements (Beiersdorfer, Decaux, & Widmann 1995). Excited ions with radiative lifetimes $\lesssim 10^{-9}$ s radiatively decay primarily within the electron beam.

We detect X-rays from EBIT using flat crystal spectrometers (FCSs; Beiersdorfer & Wargelin 1994). The dispersion planes of the FCSs are perpendicular to the electron beam in EBIT. Between EBIT and each of the FCSs is a 1 μm thick polyimide window. X-rays are detected using proportional counters with a 4 μm thick polypropylene window. The proportional counters are operated with a P-10 gas mixture (90% Ar, 10% $CH_4$) at atmospheric pressure. Apertures collimate the observed emission for a vertical divergence of ≲18 mradians. The horizontal angular width of the collected radiation overfills the angular acceptance range of the thallium hydrogen phthalate [TAP(001)] crystals used.

For the nearly monoenergetic conditions in EBIT, the rate of line formation produced via nonresonant EIE can be expressed as

$$\left\langle \frac{dI}{d\Omega} \right\rangle = \frac{\sigma(E) v(E) \int n_e(\boldsymbol{r}) n_q(\boldsymbol{r})\, d^3\boldsymbol{r}}{4\pi}, \qquad (1)$$

where $\langle dI/d\Omega \rangle$ is the $4\pi$-averaged differential line intensity in photons $s^{-1}$ $sr^{-1}$; $\sigma$ is the total cross section for producing the line and includes cascade contributions; $E$ is the relative electron-ion energy (here essentially the electron energy); $v$ is the relative electron-ion velocity (here essentially the electron velocity); $n_e$ is the electron density at position $\boldsymbol{r}$; $n_q$ is the density of ions in charge state $q$ at $\boldsymbol{r}$; and the integral is over the volume of the trap.

Following Henke et al. (1978), a line intensity measured with an FCS may be written as

$$I^{\mathrm{FCS}} = TD\psi \left[ R_\sigma \left( \frac{dI}{d\Omega} \right)_\sigma + R_\pi \left( \frac{dI}{d\Omega} \right)_\pi \right]. \qquad (2)$$

TABLE 1

UNCERTAINTIES FOR THE Fe XXIV LINE RATIO MEASUREMENTS

| Source | $\frac{3p_{3/2}-2s_{1/2}}{3p_{1/2}-2s_{1/2}}$ (percent) | $\frac{3d_{5/2}-2p_{3/2}}{3p_{1/2}-2s_{1/2}}$ (percent) | $\frac{4p_{3/2,\,1/2}-2s_{1/2}}{3p_{1/2}-2s_{1/2}}$ (percent) |
|---|---|---|---|
| Relative transmittance factor | ... | 4 | 4 |
| Relative detection efficiency factor | ... | ... | 2 |
| Line blending | ... | 5 | ... |
| Cross calibration factor | ... | ... | 8 |
| Reproducibility | 9 | 10 | 12 |
| Electron spiraling | 2 | 1 | 1 |
| Quadrature sum | 9 | 12 | 15 |

NOTE.—Uncertainties are quoted at a confidence level believed to be equivalent to a 1 $\sigma$ statistical confidence level.

$T$ accounts for the X-ray transmittances of all windows; $D$ is the detection efficiency of the proportional counter; $\psi$ is the vertical angle collected by the FCS; and $R_\sigma$ and $R_\pi$ are, respectively, the integrated crystal reflectivities for X-rays polarized perpendicular to and parallel to the dispersion plane of the FCS. Over the vertical angle collected by the FCSs, $dI/d\Omega$ may be accurately approximated as constant.

A unidirectional beam of electrons colliding with atomic or ionic targets may produce anisotropically emitted, linearly polarized radiation (Percival & Seaton 1958). The polarization factor, $P$, of the emitted radiation is defined as

$$P = \left[\left(\frac{dI}{d\Omega}\right)_\sigma - \left(\frac{dI}{d\Omega}\right)_\pi\right] \Big/ \left[\left(\frac{dI}{d\Omega}\right)_\sigma + \left(\frac{dI}{d\Omega}\right)_\pi\right], \quad (3)$$

where $(dI/d\Omega)_\sigma$ and $(dI/d\Omega)_\pi$ are measured at an observation angle perpendicular to the electron beam and are, respectively, the differential intensity of light emitted with the electric field vector parallel to and perpendicular to the electron beam direction.

Following Beiersdorfer et al. (1992), $\langle dI/d\Omega\rangle$ for an arbitrary line $a$ can be expressed as

$$\left\langle \frac{dI_a}{d\Omega}\right\rangle = \frac{I_a^{\rm FCS}}{\psi G(a)}, \quad (4)$$

where

$$G(a) = \frac{3}{2} T_a D_a \left[\left(\frac{1+P_a}{3-P_a}\right)(R_\sigma)_a + \left(\frac{1-P_a}{3-P_a}\right)(R_\pi)_a\right]. \quad (5)$$

Using equations (1) and (4), ratios of two lines, $a$ and $b$, emitted from the same charge state and simultaneously observed with the same FCS can be written as

$$\frac{\sigma_a}{\sigma_b} = \frac{G(b) I_a^{\rm FCS}}{G(a) I_b^{\rm FCS}}. \quad (6)$$

The FCSs are narrow-band devices. We carried out broadband measurements using two FCSs and cross-calibrating the FCSs. The cross-calibration factor for line $b$ is defined as

$$C(b) = \frac{I_b^{\rm FCS1}}{I_b^{\rm FCS2}} \quad (7)$$

and is determined by observing $b$ simultaneously with FCS1 and FCS2. Using equations (6) and (7), broadband measurements may be made by simultaneously observing $a$ with FCS1 and $b$ with FCS2. It is trivial to extend the above discussion to ratios involving three or more lines.

## 3. MEASUREMENT UNCERTAINTIES

Uncertainties are listed in Table 1. Uncertainties are quoted at a confidence level believed to be equivalent to 1 $\sigma$. When appropriate, systematic uncertainties are treated as random sign errors and added in quadrature with statistical uncertainties.

The transmittances of the polyimide and polypropylene windows of FCS1 were measured using a nearly monochromatic beam of X-rays. The detection efficiency of the proportional counter in FCS1 was calculated using the measured depth of the gas absorption cell and theoretical photoabsorption cross sections that are well known experimentally and theoretically (Henke, Gullikson, & Davis 1993). The estimated uncertainty in $D_a/D_b$ is the result of variations in the depth of the absorption cell due to bulging of the polypropylene window from the pressure of the P-10. The uncertainty in $T_a/T_b$ or $D_a/D_b$ is insignificant when the change in $T$ or $D$ is negligible over the wavelength range spanned by $a$ and $b$.

The measured integrated reflectivity, $R$, of the TAP crystal in FCS1 was $(0.51 \pm 0.01)(R_p + R_m)$, where $R_p$ and $R_m$ are, respectively, the calculated total integrated reflectivities of Henke et al. (1993) for an ideally perfect crystal with absorption and for an ideally mosaic crystal. $R_\sigma$ and $R_\pi$ were determined using $R = (R_\sigma + R_\pi)/2$ and calculated values of $R_\pi/R_\sigma$. To determine $R_\sigma$ and $R_\pi$, we used the average of the predicted $R_\pi/R_\sigma$ value for ideally perfect crystals with absorption (Henke et al. 1993) and ideally mosaic crystals [$R_\pi/R_\sigma = \cos^2(2\theta_{\rm B})$]. The Bragg angle, $\theta_{\rm B}$, was determined using the known wavelengths of the observed lines (Kelly 1987) and the known $2d_\infty$ spacings of TAP (Hendry & Langford 1974; Barrus et al. 1981). The uncertainty in $R$ is a systematic uncertainty and cancels out when forming line ratios. The uncertainty in $R_\pi/R_\sigma$ results in uncertainties of $\sim$4% in $R_\pi$ and $\sim$2% in $R_\sigma$, which are negatively correlated and roughly cancel out in equation (5). Thus, the uncertainties in $R_\pi$ and $R_\sigma$ have an insignificant effect on the present results.

Representative $3 \rightarrow 2$ and $4 \rightarrow 2$ spectra are shown in Figures 1 and 2. The spectra consist entirely of Fe XXII, XXIII, and XXIV lines (Kelly 1987; Wargelin et al. 1996). Spectra collected with no iron ions in EBIT were devoid of discernible features. The Fe XXIV $3p$–$2s$ and $4p$–$2s$ doublets are predicted by theory to be unblended with other Fe XXII, XXIII, and XXIV lines. Using theory, the observed Fe XXIV $3d_{5/2}-2p_{3/2}$ line was multiplied by 0.9 to account for blending with the $3d_{3/2}-2p_{3/2}$ line. The $3d_{5/2}-2p_{3/2}$ line also blends with an Fe XXIII $2s2p\ ^1P_1-2p3p\ ^1D_2$ line. Using theoretical calculations and the ionization balance in EBIT inferred from measured Fe XXIII

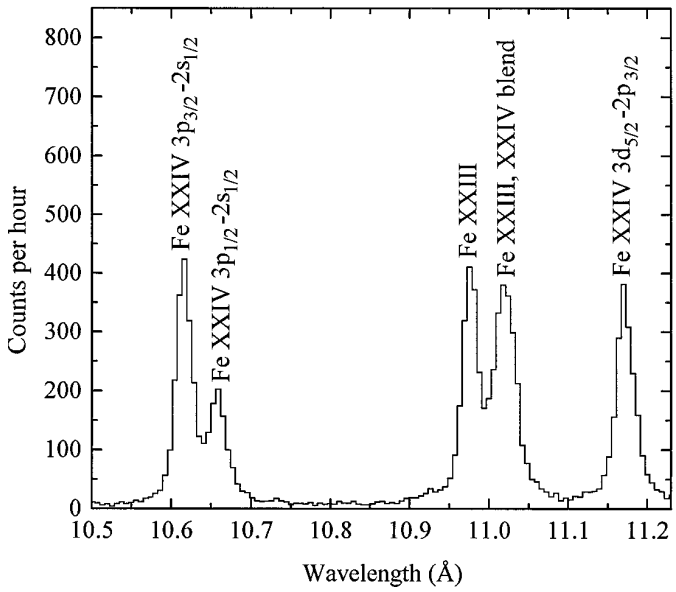


FIG. 1.—Fe XXIV $3 \rightarrow 2$ spectrum at an electron beam energy of 4500 eV recorded for 155 minutes. The spectrum was collected using a thallium hydrogen phthalate crystal in first order.

and XXIV line intensities, we estimate the effect of this blend to be negligible.

We carried out measurements for energies above the ionization threshold of Fe XXIV and below the *KLM* (i.e., $1s2l3l'$) dielectronic recombination (DR) resonances of Fe XXIV and XXV. At these energies, a significant amount of Fe XXV exists in EBIT, but neither Fe XXV nor Fe XXIV can undergo DR and produce a photon that might blend with the observed lines.

Line ratios may be affected by recombination-cascade processes such as charge transfer (CT) or radiative recombination (RR). CT populates high-$n$ levels. Observation of the Fe XXIV Rydberg series showed insignificant enhancement of $n \rightarrow 2$ photons over that predicted for EIE. We determined the effects of RR by measuring line ratios for energies spaced in 0.05 keV steps between 4.45 and 4.90 keV. The Fe XXIV *KLL* DR resonances (i.e., $1s2l2l'$) lie in this range. The Fe XXV/Fe XXIV ratio is predicted to decrease by an order of magnitude as the energy is stepped across the DR resonances. A corresponding decrease in the RR contribution to the observed Fe XXIV spectra is expected as the resonances are crossed, while the change in the EIE contribution is expected to be small. To within the reproducibility of the measurements, we saw no changes in any of the line ratios. We conclude that recombination-cascade processes have an insignificant effect on our results.

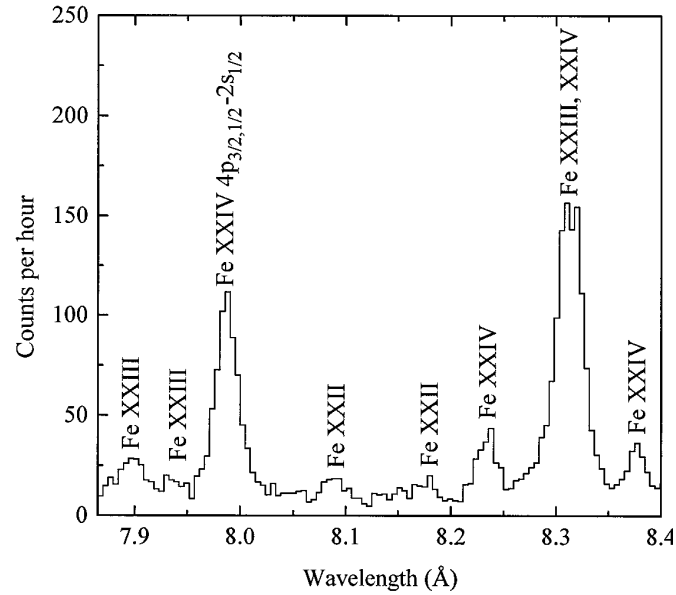


FIG. 2.—Fe XXIV $4 \rightarrow 2$ spectrum at an electron beam energy of 4500 eV recorded for 155 minutes. The spectrum was collected using a thallium hydrogen phthalate crystal in first order.

Reproducibility of the measured line ratios and of the calibration factor represents the largest uncertainty in the present results. This uncertainty is attributed to a combination of statistics, line blending, and background level and line shape determinations. Line ratio measurements require the intensity be determined for every line of interest. Here the $4p$–$2s$ doublet was unresolved. We determined the intensities of each of the $4p$ lines using the measured total intensity of the doublet and the measured $(3p_{3/2}-2s_{1/2})/(3p_{1/2}-2s_{1/2})$ ratio. The $3p$–$2s$ and $4p$–$2s$ transitions are analogous. The polarization factors for the $3p_{3/2}-2s_{1/2}$ and $4p_{3/2}-2s_{1/2}$ transitions are predicted by theory to be nearly the same, as are the $(3p_{3/2}-2s_{1/2})/(3p_{1/2}-2s_{1/2})$ and $(4p_{3/2}-2s_{1/2})/(4p_{1/2}-2s_{1/2})$ line ratios. We estimate to be insignificant the effects on the inferred $(4p_{3/2,\,1/2}-2s_{1/2})/(3p_{1/2}-2s_{1/2})$ ratio resulting from the uncertainty in the measured $(3p_{3/2}-2s_{1/2})/(3p_{1/2}-2s_{1/2})$ ratio and the different values of $\theta_B$, $R_\pi/R_\sigma$, and $R$ for the $3p$ and $4p$ doublets.

Electrons in EBIT spiral along the magnetic field lines and are not truly unidirectional. This introduces less than a 2% uncertainty in the measured and predicted line ratios.

## 4. RESULTS

Narrow-band measurements were carried out with FCS1. For broadband measurements, FCS2 was cross-calibrated to FCS1 for detection of the $3p_{1/2}-2s_{1/2}$ line. FCS1 was then used to observe the $4p_{3/2,\,1/2}-2s_{1/2}$ doublet, while FCS2 was used to observe the $3p_{1/2}-2s_{1/2}$ line. Measured line ratios are listed in Table 2.

Theoretical line ratios are also listed in Table 2. Line ratios have been calculated with the fully relativistic distorted wave (RDW) code of Zhang, Sampson, & Clark (1990) and the quasi-relativistic distorted wave atomic code HULLAC (Bar-Shalom, Klapisch, & Oreg 1988). Branching ratios are determined from radiative rates calculated with HULLAC using a multiconfiguration, relativistic, parametric potential method in intermediate coupling (Klapisch et al. 1977). Branching ratios are added to the EIE cross sections to predict line intensities. Cross sections for EIE to magnetic sublevels are calculated using the RDW code. Following Beiersdorfer et al. (1996), these RDW cross sections are used to determine polarization factors. RDW calculations include cascade contributions from all levels $n \leq 5$. Cascades from higher $n$ levels are predicted to be negligible. HULLAC calculations include cascades from all levels $n \leq 7$ (Liedahl et al. 1995).

The $(3p_{3/2}-2s_{1/2})/(3p_{1/2}-2s_{1/2})$ and $(3d_{5/2}-2p_{3/2})/(3p_{1/2}-2s_{1/2})$ line ratios predicted by RDW and HULLAC all lie within 1 $\sigma$ of the measured values. The $(4p_{3/2,\,1/2}-2s_{1/2})/(3p_{1/2}-2s_{1/2})$ line

TABLE 2

MEASURED AND PREDICTED LINE RATIOS RESULTING FROM ELECTRON IMPACT EXCITATION OF THE $2s_{1/2}$ LEVEL OF Fe XXIV

| ENERGY (keV) | $\frac{3p_{3/2}-2s_{1/2}}{3p_{1/2}-2s_{1/2}}$ | | | $\frac{3d_{5/2}-2p_{3/2}}{3p_{1/2}-2s_{1/2}}$ | | | $\frac{4p_{3/2,1/2}-2s_{1/2}}{3p_{1/2}-2s_{1/2}}$ | | |
|---|---|---|---|---|---|---|---|---|---|
| | EBIT | Theory[a] | Theory[b] | EBIT | Theory[a] | Theory[b] | EBIT | Theory[a] | Theory[b] |
| 2.50 ..... | 1.73 ± 0.16 | 1.88 | 1.89 | 2.35 ± 0.28 | 2.54 | 2.29 | ... | 0.406 | 0.362 |
| 4.50 ..... | 1.75 ± 0.16 | 1.88 | 1.81 | 1.86 ± 0.22 | 1.97 | 1.79 | 0.492 ± 0.074 | 0.409 | 0.386 |

NOTE.—Total experimental uncertainties are quoted at a confidence level believed to be equivalent to a 1 $\sigma$ statistical confidence level.
[a] RDW.
[b] HULLAC.

ratios predicted by RDW and by HULLAC lie within 1.1 $\sigma$ and 1.4 $\sigma$ of the measured value, respectively.

## 5. CONCLUSIONS

We have measured several Fe XXIV emission-line ratios with a 1 $\sigma$ uncertainty of 9%–15%. The dominant uncertainties are attributed to counting statistics, line blending, and line shape and background level determinations. These uncertainties may possibly be reduced in the future by collecting spectra with longer integration times and higher resolving power.

It is interesting to note the energy dependence of the $(3d_{5/2}-2p_{3/2})/(3p_{1/2}-2s_{1/2})$ ratio and the relative insensitivity to electron energy of the $(3p_{3/2}-2s_{1/2})/(3p_{1/2}-2s_{1/2})$ and $(4p_{3/2,1/2}-2s_{1/2})/(3p_{1/2}-2s_{1/2})$ ratios. These energy dependences, and the fact that Fe XXIV should be observable in extrasolar X-ray sources over a broad temperature range (~1–10 keV), suggest that the $(3d_{5/2}-2p_{3/2})/(3p_{3/2,1/2}-2s_{1/2})$ and $(3d_{5/2}-2p_{3/2})/(4p_{3/2,1/2}-2s_{1/2})$ ratios may be useful as temperature diagnostics. This mechanism should also work for those Li-like ions observable with *AXAF* and *XMM* (Mg, Si, S, Ar, Ca, Fe, and Ni). This will be discussed in a future paper.

Liedahl et al. (1995) report a factor of ~2 discrepancy between their calculated Fe XXIII and XXIV line ratios and the solar flare observations of McKenzie et al. (1985). Our results are for monoenergetic electrons and are not directly comparable with the observations of McKenzie et al. (1985). But our results are in good agreement with the Fe XXIV calculations. Resonances are predicted to have a negligible effect on the observed Fe XXIII and XXIV line emission. This suggests the discrepancies are most likely due to macroscopic astrophysical effects and/or the scanning technique used for broadband solar flare spectroscopic measurements which resulted in the $3 \rightarrow 2$ and $4 \rightarrow 2$ lines not being observed simultaneously.

In conclusion, our work confirms the results of the nonresonant portion of distorted wave (DW) calculations for Fe XXIV at electron energies significantly greater than the threshold energies of the transitions reported here. These calculations, however, remain to be experimentally verified for energies at which resonances may be important and for energies near threshold where DW calculations may overpredict the EIE cross section. The Fe XXIII calculations of Liedahl et al. (1995) also remain to be experimentally verified.

The authors wish to thank R. E. Marrs for discussions about EBIT; C. P. Bhalla, A. L. Osterheld, and J. H. Scofield for theoretical discussions; and S. M. Compton, E. W. Magee, and D. H. Nelson for their expert technical support. Work at Lawrence Livermore National Laboratory was performed under the auspices of the US Department of Energy (contract W-7405-ENG-48). This program is supported by the NASA High Energy Astrophysics X-Ray Astronomy Research and Analysis grant NAGW-4185.

## REFERENCES

Barrus, D. M., et al. 1981, in Low Energy X-Ray Diagnostics—1981, ed. D. T. Attwood & B. L. Henke (New York: AIP), 115
Bar-Shalom, A., Klapisch, M., & Oreg, J. 1988, Phys. Rev. A, 38, 1773
Beiersdorfer, P., et al. 1992, Phys. Rev. A, 46, 3812
Beiersdorfer, P., Decaux, V., & Widmann, K. 1995, Nucl. Instrum. Methods B, 98, 566
Beiersdorfer, P., & Wargelin, B. J. 1994, Rev. Sci. Instrum., 65, 13
Beiersdorfer, P., et al. 1996, Phys. Rev. A, 53, 3974
Drake, S. A., et al. 1994, ApJ, 436, L87
Fabian, A. C., et al. 1994, ApJ, 436, L63
Hendry, G. L., & Langford, J. I. 1974, X-Ray Spectrom., 3, 133
Henke, B. L., et al. 1978, J. Appl. Phys., 49, 480
Henke, B. L., Gullikson, E. M., & Davis, J. C. 1993, At. Data Nucl. Data Tables, 54, 181
Kaastra, J. S., & Mewe, R. 1993, Legacy, 3, 16
Klapisch, M., et al. 1977, J. Opt. Soc. Am., 67, 148
Kelly, R. L. 1987, J. Phys. Chem. Ref. Data, 16, Suppl. 1
Levine, M. A., et al. 1988, Phys. Scr., T22, 157
Liedahl, D. A., Osterheld, A. L., & Goldstein, W. H. 1995, ApJ, 438, L115
McKenzie, D. L., et al. 1985, ApJ, 289, 849
Mewe, R., Gronenschild, E. H. M. B., & van den Oord, G. H. J. 1985, A&AS, 62, 197
Percival, I. C., & Seaton, M. J. 1958, Philos. Trans. R. Soc. London, A, 251, 113
Raymond, J. C., & Smith, B. W. 1977, ApJS, 35, 419
Wargelin, B. J., et al. 1996, in preparation
White, N. E., et al. 1994, PASJ, 46, L97
Zhang, H. L., Sampson, D. H., & Clark, R. E. H. 1990, Phys. Rev. A, 41, 198